MR imaging findings of carcinoma ex pleomorphic adenoma related to extracapsular invasion and prognosis

（多形腺腫由来癌の被膜外浸潤と予後に関連する MRI画像所見）

千葉大学大学院医学薬学府

先端医学薬学専攻

（主任：宇野　隆　教授）

阿久津 陽

Abstract

Background and purpose

MRI can reflect the pathological progression of carcinoma ex pleomorphic adenoma (CXPA). This study aimed to identify the imaging findings related to extracapsular invasion of CXPA. Additionally, the pathological background of these findings was investigated.

Materials and methods

This retrospective study included 37 patients with histologically confirmed CXPA. Three radiologists independently evaluated whether the CXPA showed the following characteristic MRI findings: border, capsule, the corona sign on fat-saturated T2WI (FS-T2WI) and contrast-enhanced-fat-saturated-T1WI (CE-FS-T1WI), and the black ring sign. The corona sign appeared larger on FS-T2WI and/or CE-FS-T1WI than on T1WI. The black ring sign was defined as an intratumoral nodule with a thick low-intensity rim on T2WI. Inter-reader agreement of the visual assessment was performed using kappa analysis, and MRI and histopathological findings were also correlated. Kaplan–Meier survival and the log-rank test were used to estimate the 3-year disease-free survival.

Results

MRI findings, especially peritumoral findings, showed a significant difference between invasive and noninvasive CXPA. The reliability was poor for the border and capsule; contrastingly, it was good for the corona sign on FS-T2WI and CE-FS-T1WI and the black ring sign. Pathologically, the corona sign reflected the invasiveness of the tumor and inflammatory cells, while the black ring sign reflected hyalinization or fibrosis. The corona sign also showed a significant difference in the 3-year disease-free survival.

Conclusion

MRI findings, including the corona and black ring signs, reliably differentiated invasive and noninvasive CXPA. The corona signs can be used as a prognostic factor for CXPA.

Abbreviation Key

CE = contrast-enhanced

CXPA = carcinoma ex-pleomorphic adenoma

DFS = disease-free survival

FS = fat-saturated

PA = pleomorphic adenoma

WHO = World Health Organization

Introduction

Carcinoma ex-pleomorphic adenoma (CXPA) arises from a pre-existing pleomorphic adenoma (PA). It is more likely to occur in cases of PAs with multiple recurrences or requiring long-term follow-ups. CXPA comprises 3.6% and 11.6% of all salivary gland tumors and malignancies, respectively, and is most often found in the parotid gland.[1,2]

Carcinoma in PA develops in the luminal cells of the tubular structures, and the malignant cells then destroy the pre-existing PA structure.[3-5] CXPA is classified by the World Health Organization (WHO) as noninvasive, minimally invasive, or frankly invasive.[6] In CXPA, the carcinoma is considered non-invasive until the malignant cells are confined within the pre-existing PA capsule and invasive when the malignant cells cross over the capsule.[6,7] Noninvasive and minimally invasive CXPAs have a better prognosis and can be treated with localized resection. In contrast, frankly invasive CXPAs have a poor prognosis and require widespread resection, including the margins around the tumor.[6-8]

We hypothesized that MRI findings could reflect this pathological spectrum of CXPA. CXPA may initially resemble PA, and the imaging findings were likely to

change according to the pathological changes that occur with carcinomatous invasion. The internal components of CXPA can show various imaging findings depending on the proportions of the mucinous stroma and hyalinization/fibrosis proportions in the pre-existing PA and histological diversity of the carcinoma component.[9-10] Hence, we predicted that the imaging features of CXPA could be captured by focusing on the tumor margins rather than on its internal morphology.

Only a few case reports describing the radiologic features of CXPA have been published. A previous review showed encapsulated components with a hypointense rim on T2WI and fat-saturated (FS) T2WI in some CXPA cases, which may be a characteristic finding.[3] However, the clinical significance of this finding has not been fully investigated.

Thus, we aimed to reveal the imaging spectrum of CXPA, specifically focusing on the imaging findings reflecting invasion beyond the PA capsule. In addition, we correlated the imaging findings with the pathological background and subsequently evaluated the contribution of the imaging findings to prognostic prediction.

Materials and Methods

Study participants

This retrospective study was approved by our Institutional Review Board, and the need for written informed consent was waived.

We found 41 potentially relevant cases via a computer search of the pathological records between August 2007 and April 2020 at our institution. The following keyword was employed during the search: “carcinoma ex-pleomorphic adenoma.”

Patients were excluded for the following reasons: 1) absent or inaccessible MRI images because the MRI was performed about 15 years ago (n=1), 2) no head and neck MRI because of CXPA metastasis to the vertebral body (n=1), 3) non-standard MRI protocol (only intracranial MRI) (n=1), and 4) lack of surgical pathological confirmation (n=1). Of the 41 potential cases that were reviewed, only 37 patients who underwent surgery and had histopathologically proven CXPA were included. Five patients were aware of the mass for about 10 years but had neglected it. six were under observation because of benign or suspected

PA on fine-needle aspiration and imaging tests, and one patient had the tumor surgically removed in the past. The patients underwent multiple preoperative imaging studies at various timepoints as part of their standard care.

In our institution, all patients underwent an initial CT examination approximately 3 months after surgery, followed by CT evaluations every 6 months. If recurrence was suspected, additional imaging studies, such as MRI and FDG-PET/CT, or biopsies were performed. Patients also underwent postoperative radiation (60 Gy/30 Fx) in pathologically positive or those with close surgical margins and were histologically identified as high-grade malignancy.

MRI protocol

MR images were obtained using a 1.5T MR scanner (Signa HDxt, GE Healthcare, Milwaukee, WI, USA). The imaging protocol included axial T1WI, T2WI, FS-T2WI, and coronal T2WI sequences. Dynamic MRI, contrast-enhanced (CE)-FS-T1WI, and DWI/ADC mapping were also performed.

Image and data analysis

Clinical and prognostic data were extracted from the medical records, and MRI findings were independently evaluated by three radiologists with 6, 10, and 18 years of imaging experience, respectively. In cases involving initial disagreement, the final evaluation was decided by consensus among the three raters. Visual assessment of the tumor margins included the border and capsule. The border was evaluated using only conventional T1WI and T2WI, and the capsule was defined as the low-signal area and/or the contrast-effect area of the margin in consideration of the chemical shift artifact. The border was evaluated first, followed by the capsule. The border was assessed as well-defined, partially ill-defined, or totally ill-defined, and the capsule was assessed as complete, incomplete, or absent on a three-point scale.

In addition, the corona signs on FS-T2WI and CE-FS-T1WI and the black ring sign were evaluated. The corona sign was considered if the tumor size on FS-T2WI or CE-FS-T1WI was larger than that on T1WI **(Fig. 1)**. We defined the presence of a component encapsulated with a hypointense rim on T2WI or FS-T2WI as the black ring sign, as reported by Kashiwagi et al.[3] **(Fig. 2)**. In this study, a lesion with a hypointense rim, which was noticeably thicker than the pre-existing PA capsule, was defined as the black ring sign. Intra-ring signals

were not considered. Because the PA capsule's thickness ranges from 15 to 1750 μm, we defined lesions with >2 mm thickness as the black ring. [8]

Radiology-pathology correlation

Radiology-pathology correlation was assessed by two of the three radiologists who performed the imaging evaluations and a pathologist. The review was done with a consensus among these three individuals. In particular, we focused on peritumoral findings and the region corresponding to the black ring sign.

Statistical analyses

We sorted the raters' findings into two groups for statistical analyses. Specifically, noninvasive and minimally invasive CXPAs were categorized into the noninvasive group, and frankly invasive CXPAs were categorized into the invasive group. For each imaging assessment, Fisher's exact probability test was performed in both the invasive and noninvasive groups. Inter-reader agreement of the visual assessment was performed using kappa analysis. Kappa values were interpreted as follows: <0.40, poor to fair agreement; 0.41–0.60, moderate agreement; 0.61–0.80, substantial agreement; and 0.81–1.00, almost perfect agreement.[11] Kaplan–Meier survival and the log-rank

test were used to estimate the 3-year disease-free survival (DFS). All statistical analyses were performed using R (version 3.6.3; R Foundation for Statistical Computing, Vienna, Austria), and statistical significance was set at $P<0.05$.

Results

Clinical findings

Two of the thirty-seven patients were excluded from the CE images analysis because they had not undergone CE-MRI. 12 patients had non-invasive tumors, 25 with frankly invasive, and 0 with minimally invasive tumors. The clinical characteristics of the patients are summarized in **Table 1**. Clinical information, such as age, sex, location, laterality, swelling, pain, infection, immobility, nerve palsy, and skin infiltration, showed no significant difference in relation to extracapsular invasion.

Pathological findings

The pathological characteristics of the patients are summarized in **Table 2**. No significant difference was observed in the extracapsular invasion based on the histologic subtypes of the carcinoma.

MRI findings

The MRI findings of the border, capsule, corona sign on FS-T2WI and CE-FS-T1WI, and black ring sign were significantly different in the two groups **(Table 3)**. In the noninvasive group, the black ring sign was not observed in 11 of the 12 patients (91.7%). The black ring sign was observed with massive calcification of the left buccal region on CT in one case of maxillary CXPA; the calcification showed no signal on MRI and was mistakenly judged as the black ring sign.

Inter-rater reliability

The kappa values among the three raters are summarized in **Table 4**. The border and capsule assessments showed poor agreements; in contrast, assessments of the corona signs on FS-T2WI and CE-FS-T1WI showed substantial agreement. Assessments of the black ring sign showed near perfect agreement.

Radiology-pathology correlation

In the noninvasive group, the malignant component was completely surrounded by the PA's fibrous capsule. Additionally, there were no infiltrating tumor or inflammatory cells infiltration into the normal salivary gland tissue beyond the lesion margins in this group **(Fig. 3)**.

In the invasive group, the corona signs on FS-T2WI and CE-FS-T1WI reflected tumor and/or inflammatory cells. The tumor and/or inflammatory cells showed infiltration into the surrounding fatty tissue or salivary gland tissue. The black ring sign reflected hyalinization/fibrosis. Intra-ring components showed various cells and tissues (e.g., carcinoma cells; hyalinization/fibrosis; comedonecrosis; and epithelial, myoepithelial, and mesenchymal components) containing mucoid, myxoid, and chondroid areas. These intra-ring components had diverse ratios of mucoid, myxoid, and chondroid stroma depending on the individual case **(Fig. 4)**. Additionally, some PA components were present outside the black ring sign.

Prognosis

Significant differences were observed in the DFS for invasiveness (**Fig. 5 A**, P=0.0021). Imaging findings showed significant differences in the corona signs

on FS-T2WI and CE-T1WI. However, no difference was observed in the black ring sign (**Fig. 5 B-D**, corona signs on FS-T2WI and CE-FS-T1WI [P=0.00016 and P=0.0014, respectively], and black ring sign [P=0.31]).

Discussion

The current study yielded three main findings. First, the imaging findings (the border, capsule, corona signs on FS-T2WI and CE-FS-T1WI, and black ring sign) were significantly different between the invasive and noninvasive groups. These differences were useful for distinguishing invasiveness beyond the ex-PA capsule. Second, the corona signs on FS-T2WI and CE-FS-T1WI reflected the presence of an extracapsular tumor and/or inflammatory cells. For the black ring sign, the hypointense rim on T2WI or FS-T2WI indicated hyalinization/fibrosis, and the intra-ring components reflected various cells and tissues pathologically. Third, a significant difference in DFS was observed between the invasive and noninvasive groups, and pathological extracapsular invasion was confirmed to be a prognostic factor. In addition, the imaging findings of the corona signs on FS-T2WI and CE-FS-T1WI were also prognostic factors.

To the best of our knowledge, this study included the largest number of CXPAs and is the first to compare the imaging findings of CXPA based on the WHO's classification of invasiveness. Surgical resection is the first choice of treatment for CXPA. Partial lobectomy is indicated for noninvasive or minimally invasive CXPA localized in the superficial lobe of the parotid gland, and total parotidectomy is indicated for frankly invasive CXPA.[12] Preoperative MRI may facilitate surgical planning and prognosis prediction when seeking to manage CXPA.

Marginal information could be used to differentiate between invasive and noninvasive CXPAs. We considered that a fibrous capsule usually surrounds PA and that the appearance of invasion beyond the capsule affects the morphology of the capsule and border. However, the inter-rater reliability was poor for border and capsule findings. This poor reliability might be due to variations in the pre-existing PA. PA can present with a lobulated morphology, and even normal PA can have an incomplete capsule or no capsule. In PA of minor salivary glands, the capsule surrounding the lobules could be unclear or missing.[13,14] In addition, chemical-shift artifacts make it difficult to assess thin capsules. Conversely, the corona signs on FS-T2WI and CE-FS-T1WI and the black ring

sign showed good inter-rater reliability (**Table 4**). These findings may be useful for assessing marginal findings.

The corona signs on FS-T2WI and CE-FS-T1WI reflected pathologically extracapsular tumor and/or inflammatory cells, which could indicate invasion. The black ring sign was a highly specific finding (**Table 3**; specificity, 91.7% [11 of 12 patients] for invasive CXPA, with one case in which massive calcification was mistaken for a black ring sign. Calcification can be easily recognized in CT images, and its specificity may increase further. In the pathological evaluation, severe hyalinization/fibrosis was observed, which manifested as a hypointense rim of the black ring sign on T2WI or FS-T2WI. On MRI, the intra-ring components of the black ring sign showed various signals. Pathologically, various components, such as hyaline, mucoid, myxoid, and chondroid stroma, were present, and the proportions of these components varied in each case. The organization of PA shows various patterns and a wide range of morphological and structural diversity.[14,15] The black ring sign is suggested to reflect a pre-existing PA or a part of the existing PA. Extensive hyalinization/fibrosis has been identified as an important predictor of malignant transformation in PAs in several pathological studies. This supports our hypothesis,[16-18] and we observed

that the black ring sign effectively assessed invasiveness. If the black ring sign reflects pre-existing PA, it could be a sign of invasive CXPA.

In the survival curve, pathological invasion beyond the pre-existing PA capsule was associated with recurrence. This result was consistent with previous reports, and CXPA without extracapsular infiltration showed benign behavior.[16,19-22] Our results showing no recurrence in noninvasive cases were similar to those reported by Marino et al. and Zhao et al.[19,20] Therefore, noninvasive CXPA may be managed surgically, similar to benign PAs.

Information on the tumor margins, such as the corona signs on FS-T2WI and CE-FS-T1WI, was a prognostic finding. The black ring sign did not show a significant difference in prognosis. This is because the black ring sign had high specificity but low sensitivity to extracapsular infiltration of the CXPA (**Table 3**; sensitivity, 56% [14 of 25 patients]).

This study had some limitations. First, the histological types of the carcinomas in the CXPA varied in our study, and this variation may have affected the imaging findings. Second, only CXPA—and no other type of salivary gland tumor—was studied. Third, although CXPA has been classified into three types based on the

degree of invasiveness, this study did not include cases of minimally invasive CXPA. Minimally invasive CXPA may be overlooked because it requires pathological evaluation of all tumor margins. However, none of the cases that were actually considered noninvasive showed recurrence, and the prognosis was clearly divided between invasive and noninvasive cases. These findings indicate that a proper pathological classification was performed.

Conclusions

MRI is useful for differentiating between invasive and noninvasive CXPAs. The corona signs on FS-T2WI and CE-FS-T1WI were reliable predictors of the invasiveness of CXPA and overall prognosis. The black ring sign was also a characteristic feature of invasive CXPA. Distinction between invasive and noninvasive CXPA using preoperative MRI may contribute to surgical planning and prediction of the prognosis of CXPA.

References

1. Gnepp DR. Malignant mixed tumours of the salivary glands: a review. *Pathol Annu* 1993;28:279-328.
2. Olsen KD, Lewis JE. Carcinoma ex pleomorphic adenoma: a clinicopathologic review. *Head & Neck* 200;23:705-12. DOI: https://doi.org/10.1002/hed.1100
3. Kashiwagi N, Murakami T, Chikugo T, et al. Carcinoma ex pleomorphic adenoma of the parotid gland: *Acta Radiol* 2012;53:303-6. DOI: https://doi.org/10.1258/ar.2011.110389
4. Kato H, Kanematsu M, Mizuta K, et al. Carcinoma ex pleomorphic adenoma of the parotid gland; radiopathologic correlation with MR imaging including diffusion-weighted imaging. *Am J Neuroradiol* 2008;17:865-7. DOI: https://doi.org/10.3174/ajnr.A0974
5. Weiler C, Zengel P, van der Wal JE, et al. Carcinoma ex pleomorphic adenoma with special reference to the prognostic significance of histological progression: a clinicopathological investigation of 41 cases. *Histopathology* 2011;59:741-50. DOI: https://doi.org/10.1111/j.1365-2559.2011.03937.x

6. El-Naggar AK, Chan JKC, Grandis JR, et al. *World Health Organization classification of tumours: Pathology and genetics of head and neck tumours*. 4th edition. Lyon, France: International Agency for Research on Cancer; 2017.
7. Guzzo M, Locati LD, Prott FJ, et al. Major and minor salivary gland tumors. *Crit Rev Oncol Hematol* 2010;74:134-48. DOI: https://doi.org/10.1016/j.critrevonc.2009.10.004
8. Webb AJ, Everson JW. Pleomorphic adenomas of the major salivary glands: a study of the capsular form in relation to surgical management. *Clin Otolaryngol* 2001;26:134-42. DOI: https://doi.org/10.1046/j.1365-2273.2001.00440.x
9. Klijanienko J, El-Naggar AK, Vielh P. Fine-needle sampling findings in 26 carcinoma ex pleomorphic adenomas: diagnostic pitfalls and clinical considerations. *Diagn Cytopathol* 1999;21:163-6. DOI: https://doi.org/10.1002/(SICI)1097-0339(199909)21:3<163::AID-DC3>3.0.CO;2-2
10. Wada T, Yokota H, Horikoshi T, et al. Diagnostic performance and inter-operator variability of apparent diffusion coefficient analysis for

differentiating pleomorphic adenoma and carcinoma ex pleomorphic adenoma: comparing one-point measurement and whole-tumor measurement including radiomics approach. *Jpn J Radiol* 2020;38:207-14. DOI: https://doi.org/10.1007/s11604-019-00908-1

11. Landis JR, Koch GG. The measurement of observer agreement for categorical data. *Biometrics* 1977;33:159-74. DOI: https://doi.org/10.2307/2529310
12. Antony J, Gopalan V, Smith RA, et al. Carcinoma ex pleomorphic adenoma: a comprehensive review of clinical, pathological and molecular data. *Head Neck Pathol* 2012;6:1-9. DOI: https://doi.org/10.1007/s12105-011-0281-z
13. Margaritescu CL, Raica M, Simionescu C, et al. Tumoral stroma of salivary pleomorphic adenoma-histopathological, histochemical and immunohistochemical study. *Rom J Morphol Embryol* 2005;46:211-23.
14. de Sousa Lopes ML, Barroso KM, Henriques ÁC, et al. Pleomorphic adenomas of the salivary glands: retrospective multicentric study of 130 cases with emphasis on histopathological features. *Eur Arch*

Otorhinolaryngol 2017;274:543-51. DOI: https://doi.org/10.1007/s00405-016-4253-5

15. Margaritescu CL, Raica M, Simionescu C, et al. Tumoral stroma of salivary pleomorphic adenoma-histopathological, histochemical, and immunohistochemical study. *Rom J Morphol Embryol* 2005;46:211-23.
16. Lewis JE, Olsen KD, Sebo TJ. Carcinoma ex pleomorphic adenoma: pathologic analysis of 73 cases. *Hum Pathol* 2001;32:596-604. DOI: https://doi.org/10.1053/hupa.2001.25000
17. Auclair PL, Ellis GL. Atypical features in salivary gland mixed tumors: their relationship to malignant transformation. *Mod Pathol* 1996;9:652-7.
18. Ethunandan M, Witton R, Hoffman G, et al. Atypical features in pleomorphic adenoma-a clinico-pathologic study and implications for management. *Int J Oral Maxillofac Surg* 2006;35:608-12. DOI: https://doi.org/10.1016/j.ijom.2006.02.009
19. Mariano FV, Noronha AL, Gondak RO, et al. Carcinoma ex pleomorphic adenoma in a Brazilian population: clinico-pathological analysis of 38 cases. *Int J Oral Maxillofac Surg* 2013;42:685-92. DOI: https://doi.org/10.1016/j.ijom.2013.02.012

20. Zhao J, Wang J, Yu C, et al. Prognostic factors affecting the clinical outcome of carcinoma ex pleomorphic adenoma in the major salivary gland. *World J Surg Oncol* 2013;11:180. DOI: https://doi.org/10.1186/1477-7819-11-180
21. Masahiro S, Takashi M, Satoshi S, et al. Carcinoma ex pleomorphic adenoma of the parotid gland: A multi-institutional retrospective analysis in the Northern Japan Head and Neck Cancer Society. *Acta Otolaryngol* 2016;136:1154-8. DOI: https://doi.org/10.1080/00016489.2016.1191671
22. Katabi N, Gomez D, Klimstra DS, et al. Prognostic factors of recurrence in salivary carcinoma ex pleomorphic adenoma, with emphasis on the carcinoma histologic subtype: A clinicopathologic study of 43 cases. *Hum Pathol* 2010;41:927-34. DOI: https://doi.org/10.1016/j.humpath.2009.12.011

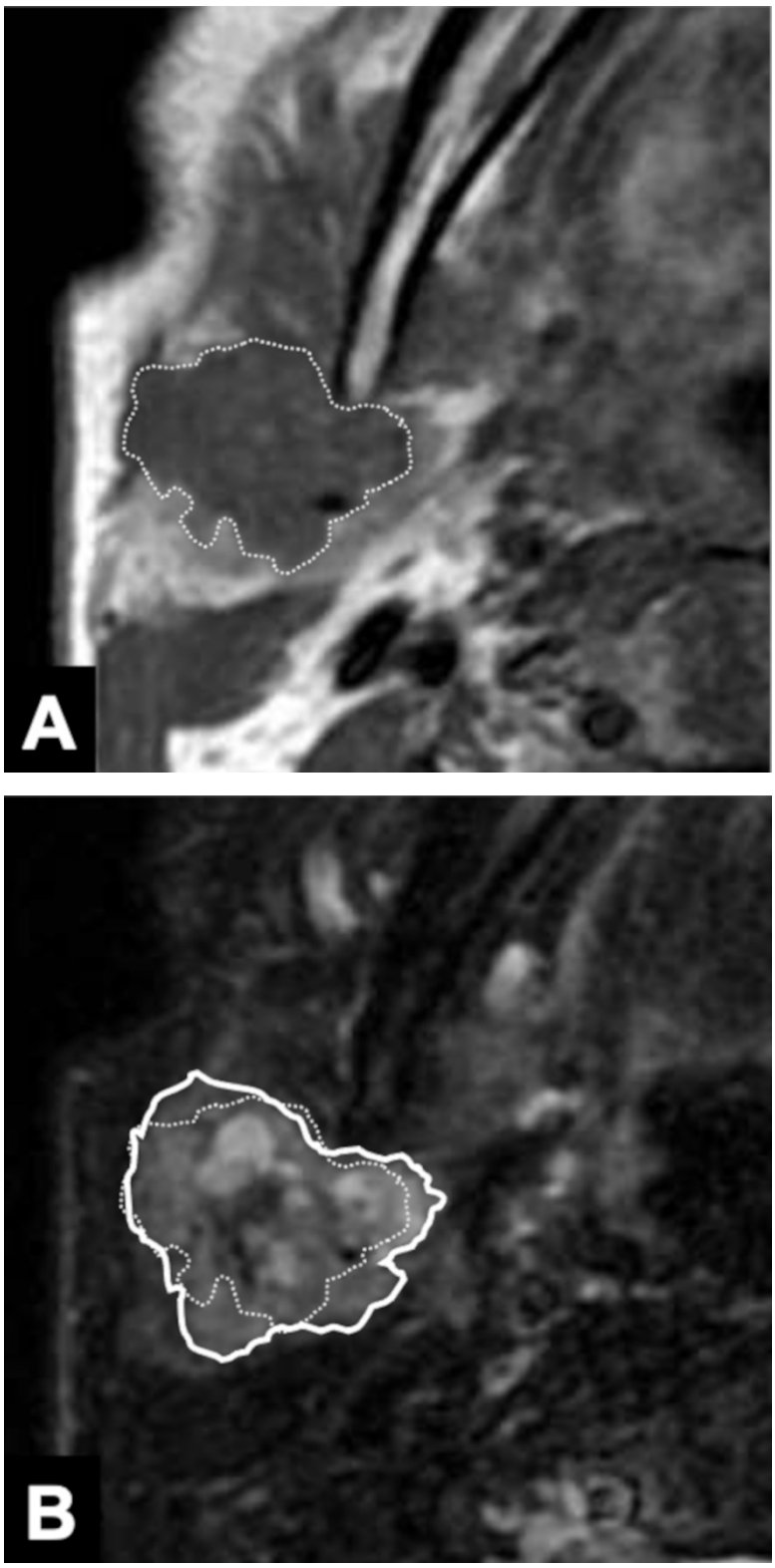
A
B

Fig. 1 Corona sign on FS-T2WI and CE-FS-T1WI

Invasive CXPA (salivary duct carcinoma) of the right parotid gland in a 77-year-old man. MRI shows a homogeneous low-intensity tumor on axial T1WI (A), mixed high- and low-intensity signals on axial fat-suppressed T2WI (FS-T2WI) (B), and irregularly enhanced signal on axial contrast-enhanced-FS-T1WI (CE-FS-T1WI) (C). The tumor size on FS-T2WI and CE-FS-T1WI (solid line) was larger than that on T1WI (dotted line). We defined these MRI findings as corona signs on FS-T2WI and CE-FS-T1WI.

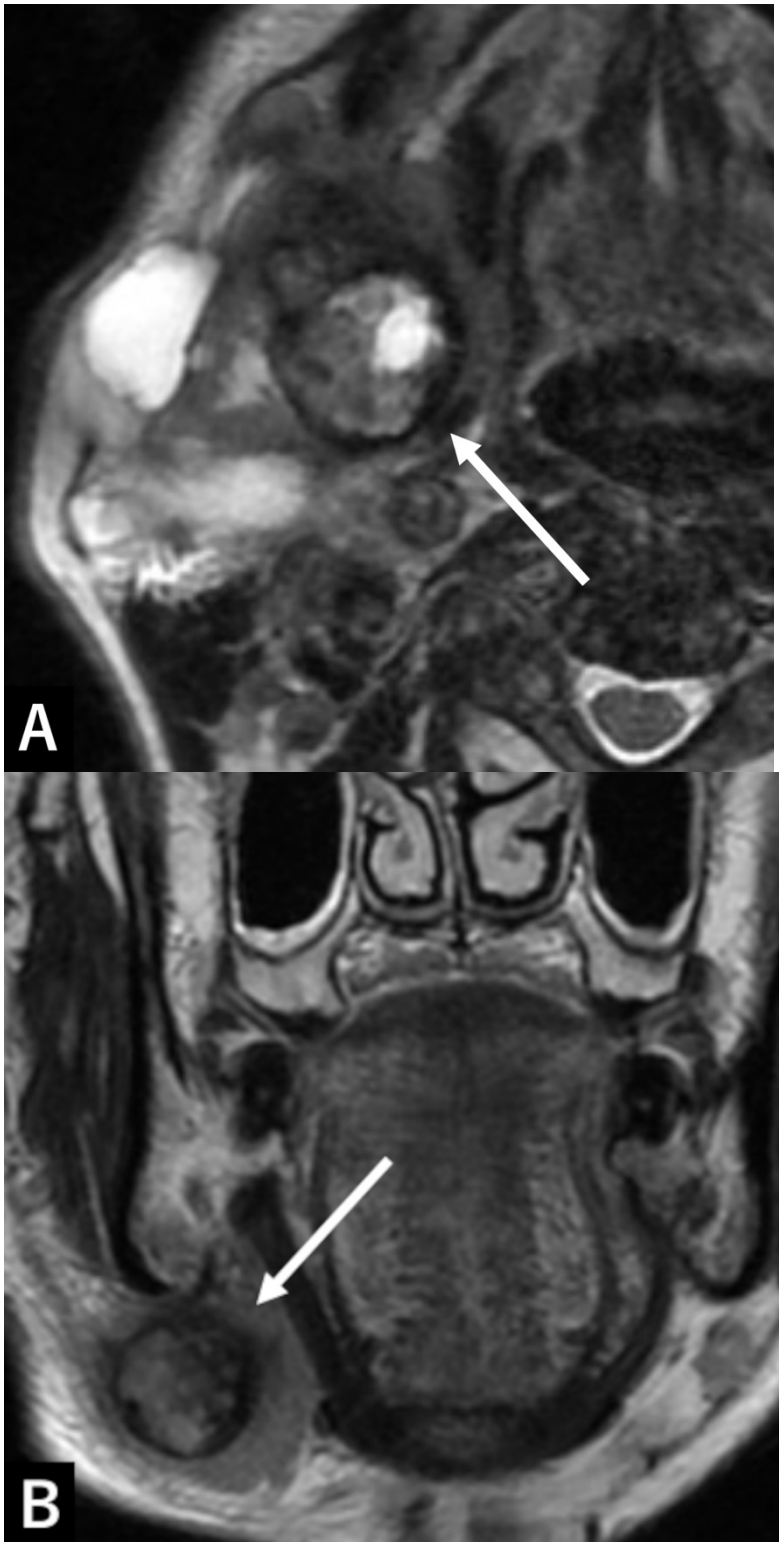

Fig. 2 Black ring sign

Invasive CXPA (high-grade mucoepidermoid carcinoma) of the right submandibular gland in a 76-year-old man. MRI shows a nodule with a thick low-intensity rim (A–B arrows) and an intra-ring component with mixed high- and low-intensity signals on axial and coronal T2WI (A-B). We defined this MRI finding as the black ring sign.

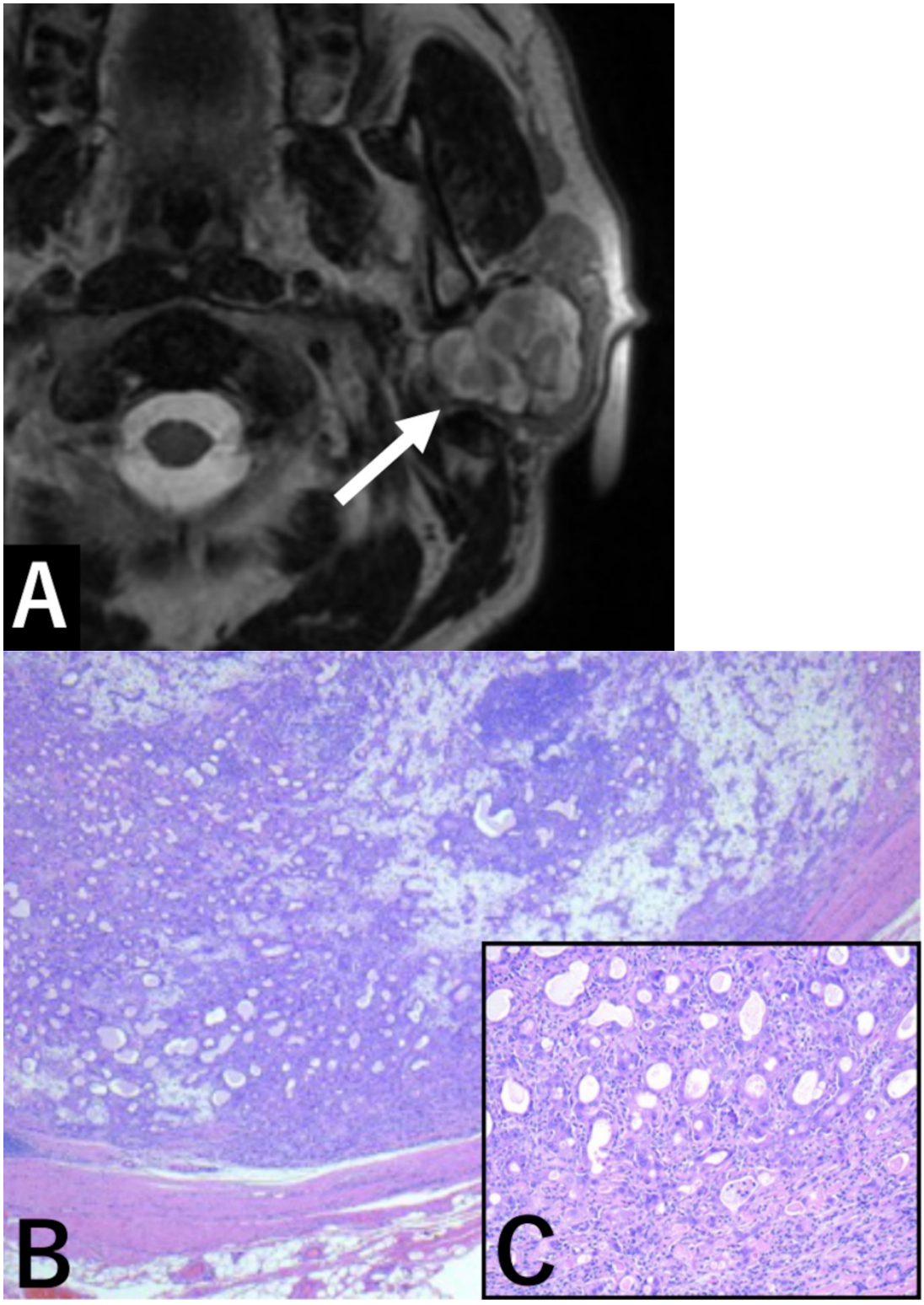

Fig. 3 MRI-pathology correlation: non-invasive type

Noninvasive CXPA (salivary duct carcinoma) of the left parotid gland in a 56-year-old man. MRI showed a heterogeneous high-intensity tumor on axial T2WI (A). There were no findings of the corona signs on FS-T2WI and CE-FS-T1WI and black ring sign. Photomicrograph showing ductal and myoepithelial cells in the chondromyxoid stroma. A part of the tumor contained ductal and myoepithelial cells with atypical hyperchromatic nuclei. The malignant component was completely surrounded by the fibrous capsule of the pre-existing pleomorphic adenoma (B: H&E ×20). Higher magnification of the malignant component (C: H&E ×100).

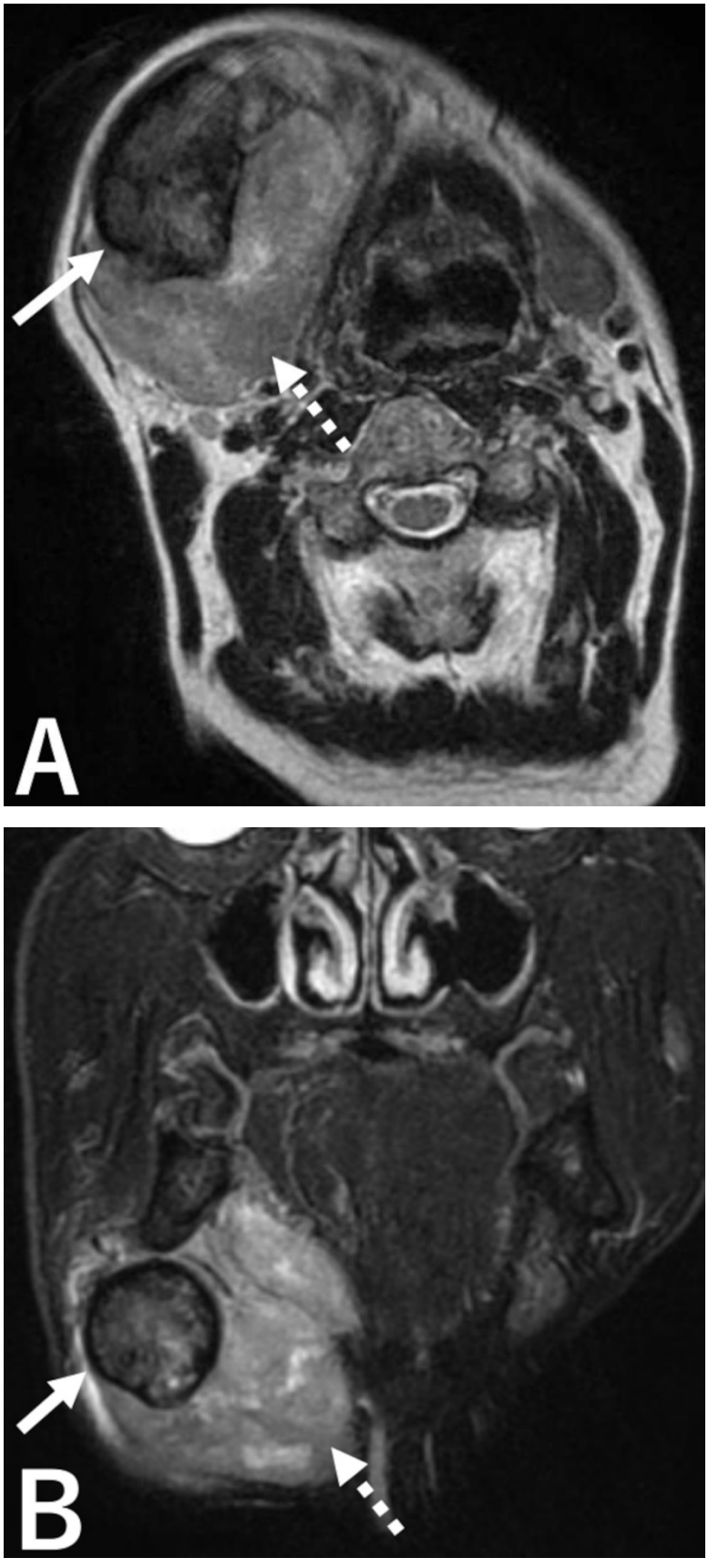
A
B

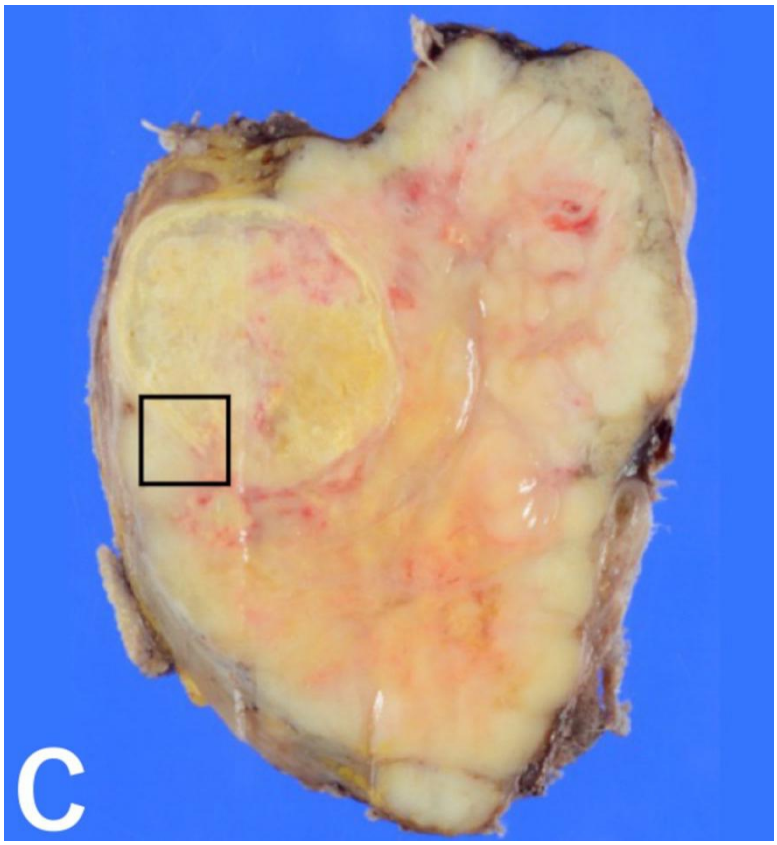
C

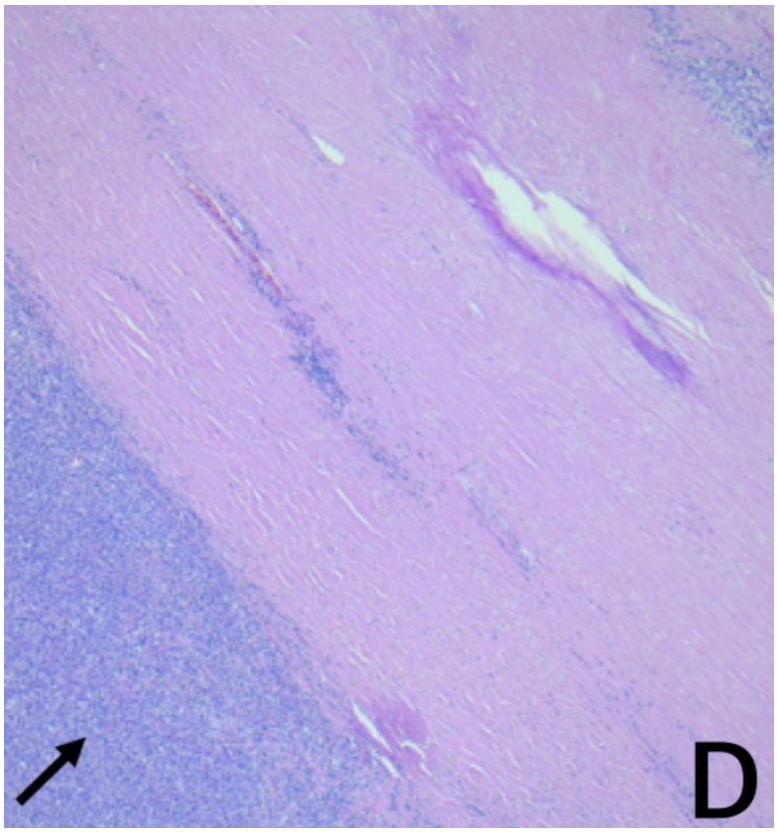
D

Fig. 4 MRI-pathology correlation: invasive type

Invasive CXPA (undifferentiated carcinoma, large cell type) of the right submandibular gland in a 72-year-old man. A huge mass replaced the right submandibular gland. MRI shows heterogeneous high-intensity on T2WI and FS-T2WI (A–B dotted arrows). Encapsulated nodules with thick low-intensity rims are present inside the tumor on axial T2WI and FS-T2WI (A–B solid arrows). Macroscopic findings showed a solid and white-yellow tumor with nodules in the nodule pattern. The nodule within the tumor corresponds to a black ring sign on MRI (C). Photomicrograph showing ductal and myoepithelial cells with atypical hyperchromatic nuclei (D: H&E ×20). The malignant component invaded beyond the capsule (D, arrows) and infiltrated into the surrounding fatty tissue. The majority of nodules within the tumor showed extensive hyalinization/fibrosis with myxoid stroma (D), and the black ring sign matched the hyalinization/fibrosis. The corona sign on FS-T2WI and CE-FS-T1WI reflects pathologically extracapsular tumor cells and/or inflammatory cells.

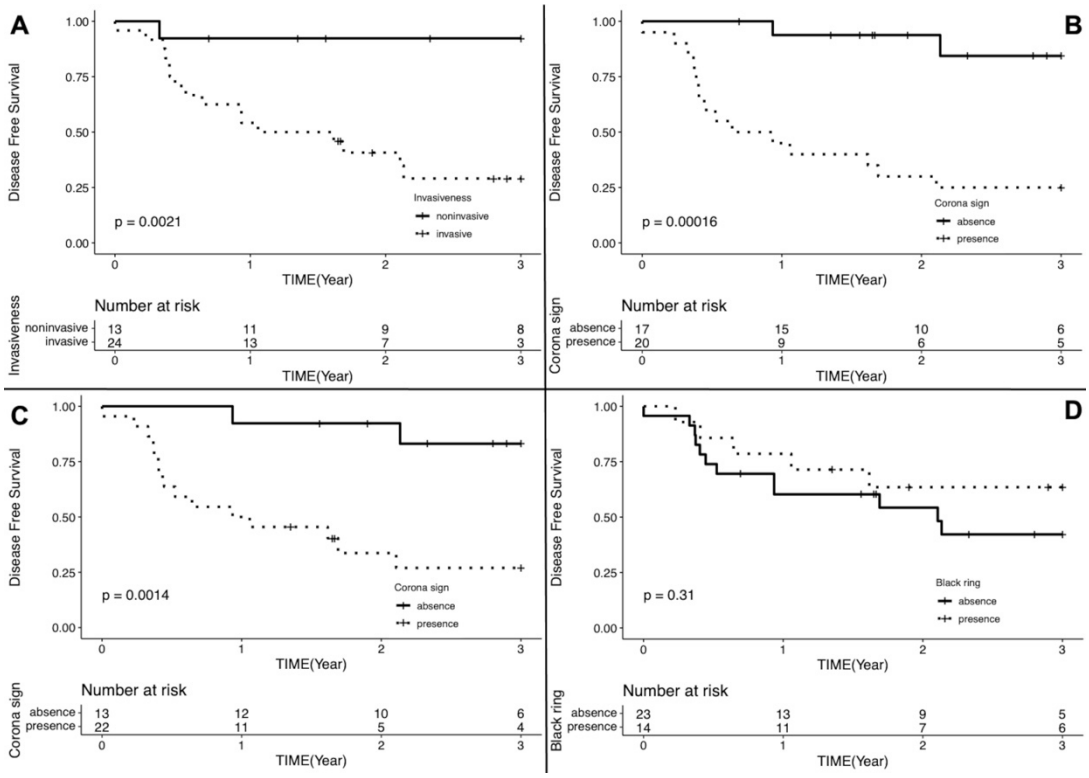

Fig. 5 Kaplan–Meier curves of disease-free survival

Table 1. Clinical characteristics of CXPA

		Total	Invasive	Non-invasive	P-value
Age		65.3±13.2	66.6±11.9	62.7±15.3	0.18
Sex	Male	26	19	7	0.28
	Female	11	6	5	
Location	Parotid	25	16	9	0.57
	Submandibular	7	6	1	
	Minor salivary	5	3	2	
Laterality	Left	17	9	8	0.08
	Right	20	16	4	
Swelling	Yes	32	20	12	0.15
	No	5	5	0	
Pain	Yes	13	10	3	0.71
	No	24	15	9	
Infection	Yes	2	2	0	1

	No	35	23	12	
Immobility	Yes	12	10	2	0.26
	No	25	25	10	
Nerve palsy	Yes	6	6	0	0.08
	No	31	19	12	
Skin infiltration	Yes	1	1	0	1
	No	36	24	12	

Table 2. Pathological characteristics of CXPA

		Total	Invasive	Non-invasive	P-value
Pathology	Salivary duct	18	11	7	0.85
	Myoepithelial	5	5	1	
	Adenocarcinoma	3	3	0	
	Squamous	3	1	2	
	Mucoepidermoid	2	2	0	
	Undifferentiated	1	1	0	
	Unknown	4	2	2	

Table 3. Imaging findings of CXPA

		Total	Invasive	Non-invasive	P-value	OR 95%CI
Border	Totally ill-defined	2	2	0	**0.002**	**14.41 [2.23-171.2] ****
	Partially ill-defined	19	17	2		
	Well-defined	16	6	10		
Capsule	None	9	9	0	**0.001**	**38.18 [4.06-1956.7] *****
	Partial	12	11	1		
	Total	16	5	11		
Corona sign on FS-T2WI	Present	21	19	2	**0.001**	**14.40 [2.23-171.2]**
	Absent	16	6	10		
Corona sign on CE-FS-T1WI*	Present	22	19	3	**0.007**	**9.31 [1.55-76.4]**
	Absent	13	5	8		
Black ring sign	Present	15	14	1	**0.011**	**13.11 [1.49-642.2]**
	Absent	22	11	11		

OR=odds ratio, CI=confidence interval

P-values < 0.05 are shown in bold.

*Two cases lacked contrast-enhanced images.

** These ORs and 95% CI were calculated between the two groups as well-defined vs. totally ill-defined and partially ill-defined.

*** These ORs and 95% CI were calculated between the two groups as none and partial vs. total.

Table 4. Inter-rater reliability of visual assessment (kappa value)

	Rater 1 vs. 2	Rater 1 vs. 3	Rater 2 vs. 3
Border	0.12	0.10	0.45
Capsule	0.19	0.38	0.16
Corona sign on FS-T2WI	0.78	0.79	0.67
Corona sign on CE-FS-T1WI	0.65	0.78	0.65
Black ring sign	0.89	0.84	0.84

Raters 1, 2, and 3 had 6, 10, and 18 years of experience, respectively.

Supplement Figure.

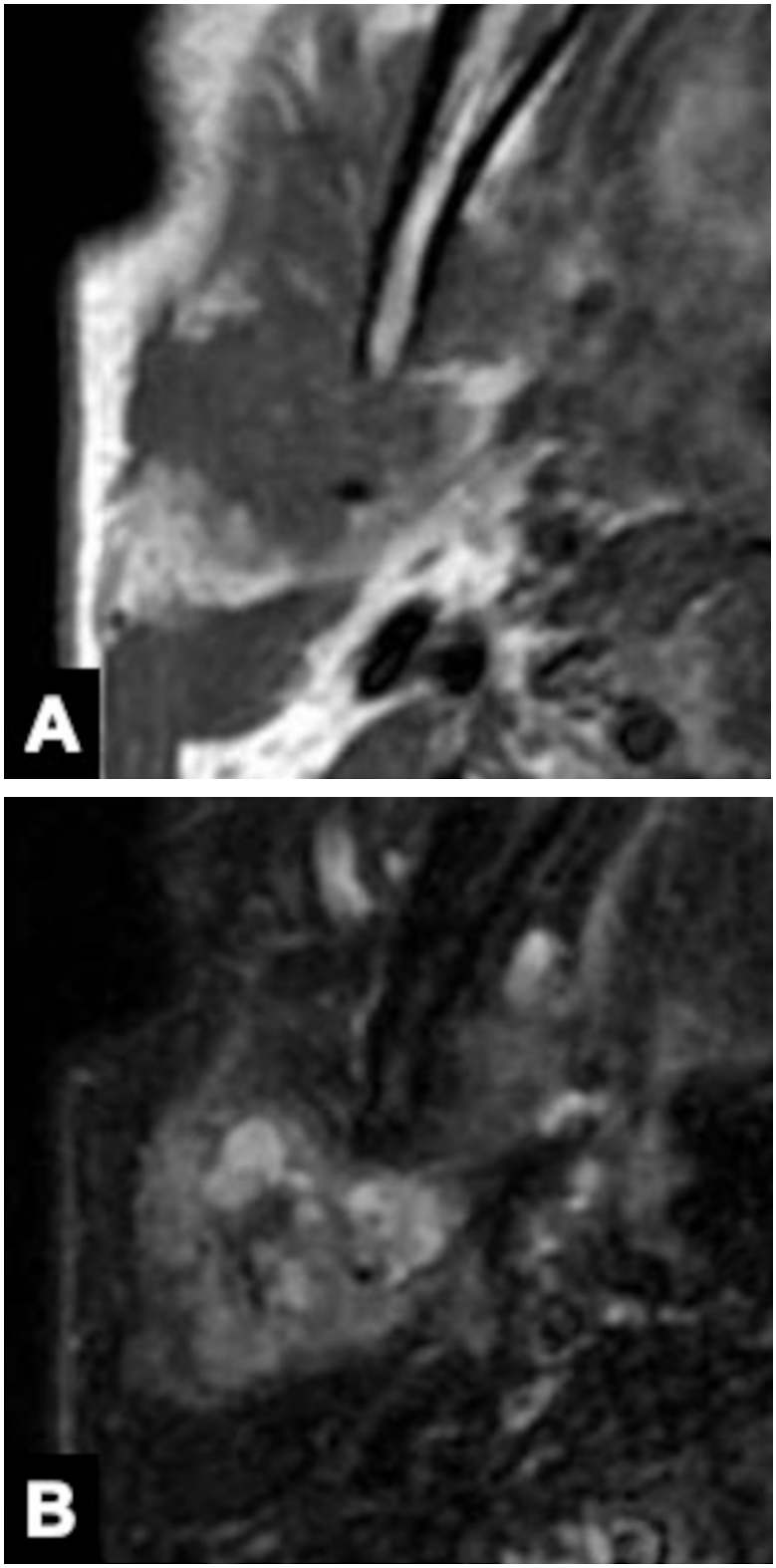
A
B

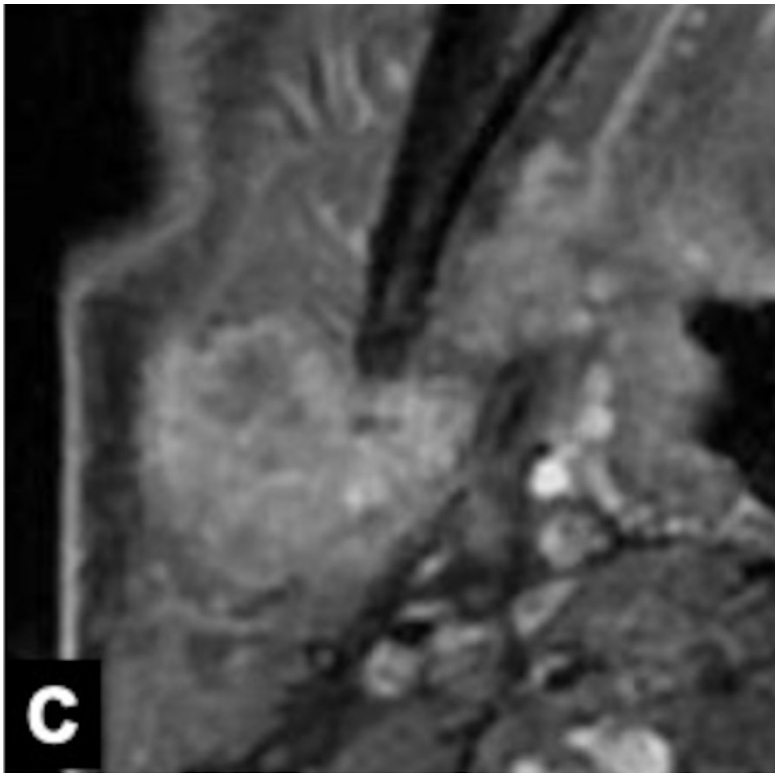

Fig. 1’ Corona sign on FS-T2WI and CE-FS-T1WI
Invasive CXPA (salivary duct carcinoma) of the right parotid gland in a 77-yearold
man. MRI shows a homogeneous low-intensity tumor on axial T1WI (A), mixed high- and low-intensity signals on axial fat-suppressed T2WI (FS-T2WI) (B), and irregularly enhanced signal on axial contrast-enhanced-FS-T1WI (CEFS-
T1WI) (C). The tumor size on FS-T2WI and CE-FS-T1WI was larger than that on T1WI. We defined these MRI findings as corona signs on FS-T2WI and CE-FS-T1WI.

Supplement Table. Image evaluation for each evaluator

Border	Rater1	Rater2	Rater3
Case 1	0	0	1
Case 2	0	0	0
Case 3	1	1	2
Case 4	0	1	0
Case 5	1	1	2
Case 6	2	2	2

Case 7	1	1	2
Case 8	1	1	2
Case 9	0	0	1
Case 10	1	1	2
Case 11	1	1	1
Case 12	0	1	1
Case 13	1	1	1
Case 14	0	0	0
Case 15	1	1	2
Case 16	1	1	2
Case 17	0	1	1
Case 18	0	0	1
Case 19	1	1	1
Case 20	0	0	1
Case 21	1	2	2
Case 22	1	1	2
Case 23	1	2	2
Case 24	0	1	2
Case 25	2	2	2
Case 26	0	1	1
Case 27	1	1	0
Case 28	1	2	2
Case 29	0	0	1
Case 30	0	1	1
Case 31	1	1	2
Case 32	1	2	1
Case 33	0	0	1
Case 34	1	2	2
Case 35	0	0	1
Case 36	0	1	2
Case 37	1	1	1

(0:well defined, 1:partially ill-defined, 2:totally ill-defined)

Capsule	Rater1	Rater2	Rater3
Case 1	0	0	1

Case 2	0	0	0
Case 3	2	1	2
Case 4	0	1	0
Case 5	2	1	2
Case 6	2	2	2
Case 7	2	1	2
Case 8	2	1	2
Case 9	0	1	1
Case 10	1	1	2
Case 11	0	1	0
Case 12	2	2	2
Case 13	2	1	2
Case 14	0	1	0
Case 15	1	2	2
Case 16	1	1	2
Case 17	1	1	1
Case 18	0	1	1
Case 19	1	1	1
Case 20	0	0	1
Case 21	2	2	2
Case 22	1	2	2
Case 23	1	2	1
Case 24	1	2	2
Case 25	1	2	2
Case 26	0	2	1
Case 27	0	1	0
Case 28	2	2	2
Case 29	0	0	1
Case 30	0	1	1
Case 31	0	1	2
Case 32	0	1	1
Case 33	1	0	1
Case 34	1	1	1
Case 35	0	0	0
Case 36	0	0	1

Case 37	1	1	1

(0:none, 1:partial, 2: total)

Black ring sign	Rater1	Rater2	Rater3
Case 1	0	0	0
Case 2	0	0	0
Case 3	1	1	1
Case 4	0	0	0
Case 5	1	1	1
Case 6	1	1	1
Case 7	1	1	1
Case 8	0	0	0
Case 9	0	0	0
Case 10	1	1	1
Case 11	0	0	0
Case 12	0	0	0
Case 13	1	1	1
Case 14	0	0	0
Case 15	1	1	1
Case 16	0	0	0
Case 17	0	0	0
Case 18	0	0	0
Case 19	1	1	1
Case 20	0	0	1
Case 21	1	1	1
Case 22	1	1	1
Case 23	1	1	1
Case 24	1	1	1
Case 25	0	1	1
Case 26	0	0	0
Case 27	0	0	0
Case 28	0	0	0
Case 29	0	0	0

Case 30	0	1	0
Case 31	1	1	1
Case 32	0	0	0
Case 33	0	0	0
Case 34	0	1	1
Case 35	0	0	0
Case 36	1	1	1
Case 37	1	1	1

(0:absent, 1:present)

Corona sign on FS-T2WI	Rater1	Rater2	Rater3
Case 1	0	0	0
Case 2	0	0	0
Case 3	1	1	1
Case 4	0	0	0
Case 5	1	1	1
Case 6	1	1	1
Case 7	1	1	1
Case 8	1	1	1
Case 9	0	0	0
Case 10	0	1	0
Case 11	0	0	0
Case 12	0	0	0
Case 13	0	1	1
Case 14	0	0	0
Case 15	0	1	1
Case 16	1	1	1
Case 17	0	1	0
Case 18	0	0	0
Case 19	1	1	1
Case 20	1	1	1
Case 21	1	1	1
Case 22	1	1	1

Case 23	1	1	1
Case 24	1	1	1
Case 25	1	1	1
Case 26	1	1	1
Case 27	1	1	0
Case 28	1	1	1
Case 29	0	0	0
Case 30	1	1	1
Case 31	1	1	1
Case 32	1	1	0
Case 33	0	1	0
Case 34	1	1	1
Case 35	0	0	0
Case 36	0	1	0
Case 37	1	1	1

(0:absent, 1:present)

Corona sign on CE-FS-T1WI	Rater1	Rater2	Rater3
Case 1	0	0	0
Case 2	0	1	1
Case 3	1	1	1
Case 4	0	0	0
Case 5	1	1	1
Case 6	1	1	1
Case 7	1	1	1
Case 8	1	1	1
Case 9	0	0	0
Case 10	0	1	0
Case 11	1	0	0
Case 12	0	0	0
Case 13	0	1	1
Case 14	0	0	0
Case 15	1	1	1

Case 16	1	1	1
Case 17	0	1	0
Case 18	0	0	0
Case 19	1	1	1
Case 20	1	1	1
Case 21	2	2	2
Case 22	1	1	1
Case 23	1	1	1
Case 24	1	1	1
Case 25	1	1	1
Case 26	1	1	1
Case 27	1	1	0
Case 28	1	1	1
Case 29	0	0	0
Case 30	1	1	1
Case 31	1	1	1
Case 32	1	1	1
Case 33	0	1	0
Case 34	1	1	1
Case 35	2	2	2
Case 36	0	0	0
Case 37	1	1	1

(0:absent, 1:present, 2:lack of contrast-enhanced images)

American journal of neuroradiology 43(11),1639-1645(November 2022)
2022年10月6日　公表済
DOI : 10.3174/ajnr.A7656